

# Deposition of Environmental Friendly Tantalum and Chromium Nitride Coatings Using HIPIMS-MPP-PEMS Technologies

*S.L. Lee, M. Cipollo, and F. Yee, U.S. Army ARDEC-Benét Labs, Watervliet, NY;  
R. Wei and K. Coulter, Southwest Research Institute, San Antonio, TX; and  
J. Lin, W. Sproul, and J.J. Moore, Colorado School of Mines, Golden, CO*

## ABSTRACT

Electroplated high contraction chrome (HC Cr) has been used for decades as protective coatings for engineering components against wear, erosion, and corrosion for cycle life extension. It is deposited on the external surfaces of engineering components as well as on the interior surfaces of cylindrical structures. In addition to the hexavalent chrome problem, HC Cr is characterized by extensive cracks which accelerate crack growth and propagation, coatings deterioration and delamination, resulting in component failures. In this work, High Power Impulse Magnetron Sputtering (HIPIMS), Modulated Pulsed Power (MPP), and a Plasma Enhanced DC Magnetron (PEMS) technologies were tested to deposit environmental-friendly Ta and CrN coatings, as potential alternatives to electroplated HC Cr. Ta coatings were deposited in planar and cylindrical geometries for high temperature wear and erosion applications. Hard and corrosion-resistant CrN coatings were deposited in planar geometry for wear and corrosion applications. Metallography, SEM, XRD phase and residual stress, Microscratch, RC indentation and Pulse Laser Heating adhesion tests, pin-on-disc wear test were performed to characterize the coatings.

## INTRODUCTION

The development of high power impulse magnetron (HIPIMS) demonstrated that a high degree of ionization of target material can produce improved dense quality films with improved morphology at relatively low deposition temperatures [1-4]. Modulated pulse power (MPP) is a variation of HIPIMS that utilizes a high pulsed peak target power density for a short period of time on the target to achieve the enhanced ionization for a higher deposition rate [5-6]. Plasma enhanced DC magnetron (PEMS) utilizing an external filament source demonstrated increased current density can deposit films of superior properties compared to conventional DC magnetron sputtering (DCMS) [7, 8].

Chromium has the same crystalline structure as A723 steel with excellent lattice parameter match (Fe-2.8665Å; Cr-2.8847Å). It has excellent adhesion to substrate steel. However, it is hard and brittle, and possesses extensive cracks to accelerate coating delamination, substrate wear, erosion, corrosion, causing component failures. Refractory metal tantalum has attractive chemical, mechanical, thermal properties: high

melting point temperatures, inert to propellant gases, good thermal conductivity and elastic modulus. Ta is formed in a stable body centered cubic (bcc Ta- 3.298Å, also known as  $\alpha$ -Ta) structure and a meta-stable tetragonal structure (also known as  $\beta$ -Ta). Bcc  $\alpha$ -Ta is soft and ductile compared to hard  $\beta$ -Ta and electroplated high contraction (HC) Cr, making it far less susceptible to crack formation and failure.

Chromium nitride, on the other hand, has high hardness, good modulus of elasticity, low coefficient of friction, and excellent properties against wear, corrosion, oxidation, abrasion. It is being studied to coat exterior surfaces of components. Chrome nitride generally forms in face-centered-cubic (fcc CrN, lattice parameter 4.14 angstroms) and hexagonal Cr<sub>2</sub>N crystalline structures. In magnetron sputtering, the formation of CrN and Cr<sub>2</sub>N depends on the nitrogen to argon concentrations in the reactive sputtering process. A very thin chromium interface layer can improve adhesion of chromium nitride to steel substrates.

Magnetron deposition processes and coating properties have been investigated for Cr [9, 10], Ta [11-21], and CrN [22-25] coatings. In this work, High Power Impulse Magnetron (HIP-IMS), Modulated Pulsed Power (MPP), Plasma Enhanced DC magnetron sputtering (PEMS) were investigated to deposit environmental friendly Ta and CrN coatings. The new technologies demonstrated that dense, adhesive, crack-resistant coatings with improved morphology can be deposited superior to DC magnetron (DCMS) coatings and electroplated HC Cr coatings with extensive cracks.

## INSTRUMENTATION AND EXPERIMENTAL CONDITIONS

A close field unbalanced magnetron system powered with either a DC or a Zpulsor Axis-180™ MPP power supply [22] was used to deposited environmental friendly Ta and CrN coatings. The substrates were A723, 1020 and 440C tool steels. Substrates were cleaned ultrasonically first in acetone and then in ethylene; then sputter etched at -650V, 200 kHz, and 1.0  $\mu$ s reverse time for 40 min using conventional pulsed DC power. Prior to CrN deposition, a Cr interface layer (300-500 nm) was deposited to enhance adhesion between coatings and substrate. By using relatively long pulses on the order of 1-3 ms and controlling the peak power-current of the pulse, it can

Table 1: Planar magnetron Tantalum deposition using MPP technology.

| Sample No. | Pa [kW] | Pp [kW] | Ia [A] | Ip [A] | Va [V] | Vp [V] | Pressure [mTorr] | Flow Rate [sccm] | Bias [V] | f [Hz] | Substrate distance [mm] | Time [hr] | Coating Thickness [ $\mu\text{m}$ ] | Ta phase                 | Hardness [GPa] | Residual Stress [ksi] |
|------------|---------|---------|--------|--------|--------|--------|------------------|------------------|----------|--------|-------------------------|-----------|-------------------------------------|--------------------------|----------------|-----------------------|
| Ta-1       | 5       | 42      | 49     | 91     | 464    | 566    | 5                | 61               | -50      | 135    | 140                     | 4         | 50                                  | $\alpha$ +little $\beta$ | 12.9           | -405 ksi              |
| Ta-2       | 4.5     | 40      | 45     | 86     | 473    | 563    | 5                | 62               | F        | 130    | 100                     | 7         | 95                                  | $\alpha$                 | 8.5            | -307ksi               |
| Ta-3       | 3.0     | 56      | 67     | 132    | 460    | 552    | 5                | 62               | -50      | 57     | 100                     | 15        | 100                                 | $\alpha$                 | 9.2            |                       |

(1) f: pulse frequency; (2)  $P_a$  and  $P_p$ : Average and peak target powers; (3)  $V_a$  and  $V_p$ : average and peak target voltages; (4)  $I_a$  and  $I_p$ : average and peak target currents.

achieve a high deposition rate while at the same time achieving a high degree of ionization of the sputtered material. In Table 1, examples of MPP deposited Ta samples are shown; in Table 3 examples of MPP deposited CrN samples are shown. Ta coatings up to 100  $\mu\text{m}$  were successfully deposited using floating or -50 volt substrate bias voltage. Thick CrN coatings up to 55 micrometer using Ar/N<sub>2</sub> ratio of 1:1 were successfully deposited at -50 volt substrate bias voltage. General systems parameters were 3-5 kW average power, 40-100 kW peak power, 40-95 A average ion current, 80-200 A peak ion current, deposition rate  $\sim$ 10-15  $\mu\text{m/hr}$ .

Plasma enhanced magnetron (PEMS) technology using an external filament can increase the ion current density 25 folds compared to conventional DCMS to deposit improved Ta coatings. PEMS coatings up to 200  $\mu\text{m}$  demonstrated success in high temperature wear and erosion tests [19, 20]. A Huettinger HMP1/1-P10-H05 HIPIMS power supply with an output of 1 kV at 1000A (1 MW peak), average power 10kW was implemented in both planar and cylindrical geometries at SWRI to test Ta and CrN depositions. A plasma-enhanced cylindrical magnetron system constructed at SWRI used two magnet designs: rectangular magnets oscillating around the cylindrical circumference and ring magnets oscillating vertically along the cylinder axis for uniform coating deposition. In Table 2, deposition parameters and characterization results are listed for Ta coatings deposited in the cylindrical geometry. Thick Ta coatings up to 200  $\mu\text{m}$  have recently been deposited on 1-ft long 120 mm barrel sections using the plasma enhanced cylindrical magnetron.

A plasma-enhanced cylindrical magnetron was implemented by the addition of substrate biasing through anode ring design and the acquisition of a Zpulsor Axis-180™ MPP power supply with 100 KW peak pulse power to the 1 ft long conventional DC cylindrical magnetron system at Benét. The system was used to deposit thick Ta coatings on the interior surfaces of 120 mm cylinders. Two cylinder sections were deposited respectively at -40 volt and at ground substrate bias using the MPP power supply.

A Hiden Analytical Electrostatic Quadrupole (EQP) mass spectrometer was used to measure the mass and ion distribution in the plasma. A Scintag PTS and a Bruker D8 diffractometers with Cu radiation were used for XRD phase analysis. A TEC X-ray stress analyzer with a Cr tube was used for residual stress analysis. Hardness measurements were made using diamond indenters. An SEM was used to obtain topography, microstructure, and coatings thickness. Nondestructive thickness mapping was performed in the cylindrical structure using a Karl Deutsch Thickness Gauge. This gauge measures ferromagnetic material based on magnetron induction principle and non-ferromagnetic substrate using Eddy current principle. The wear resistance of the CrN coatings was evaluated by a ball-on-disk microtribometer in an ambient atmosphere by sliding against a 1 mm WC-Co ball at a velocity of 25 mm/sec. The normal load applied on the sample surface was  $3\pm 0.2\text{N}$ . The average coefficient of friction (COF) values were read from the steady sliding state during the tests.

Table 2: Cylindrical magnetron tantalum deposition using DC and HIPIMS technology.

| Sample No. | Method     | Deposition |        |               |           |            |          |                          |           |        |                          |                              | Characterization |        |                                  |            |       |              |
|------------|------------|------------|--------|---------------|-----------|------------|----------|--------------------------|-----------|--------|--------------------------|------------------------------|------------------|--------|----------------------------------|------------|-------|--------------|
|            |            | Time (h)   | DC     |               | HIPIMS    |            |          |                          | Tube Bias |        |                          | Thick-ness ( $\mu\text{m}$ ) |                  |        | Deposit rate ( $\mu\text{m/h}$ ) | Hard (GPa) | Phase | Stress (ksi) |
|            |            |            | P (kW) | Ave Pwr (kVA) | V set (V) | P pk (kVA) | I pk (A) | jb (mA/cm <sup>2</sup> ) | Vb (V)    | Ib (A) | jb (mA/cm <sup>2</sup> ) | Top                          | Center           | Bottom |                                  |            |       |              |
| Tacms-1    | DC CMS     | 4          | 2.5    | -             | -         | -          | -        | -                        | -         | -      | 5.28                     | 4.6                          | 39.6             | 9.9    | 5.1                              | -Ta        | -226  |              |
| Tacms-2    | DC CMS     | 4          | 2.5    | -             | -         | -          | -        | -                        | 50        | 5.34   | 4.7                      | 37.2                         | 9.3              | 7.9    | -Ta                              | -228       |       |              |
| Tacms-3    | HIPIMS CMS | 4          | -      | 2.5           | 845       | -12        | 150      | 130.7                    | 50        |        |                          | 35.4                         | 8.9              | 11.6   | (-+)-Ta                          | -271       |       |              |
| Tacms-4    | HIPIMS CMS | 4          | -      | 2.5           | 950       | -12        | 114      | 99.3                     | -         |        |                          | 27.6                         | 6.9              | 6.6    | -Ta                              | -264       |       |              |

## RESULTS AND DISCUSSION

### Ta depositions in planar geometry using MPP technology

In Table 1, deposition parameters and characterization results are given for example Ta depositions using MPP generated plasma. In Figure 1, the mass-ion intensity of DC and MPP powered plasma at 5 mTorr argon pressure is shown. The data was obtained by placing an EQP probe in the unbalanced magnetron vacuum chamber. The data showed that using the MPP power supply, ionization of the Ta target resulted in strong  $\text{Ta}^{+1}$  and  $\text{Ta}^{+2}$  ion concentrations with higher intensity compared to  $\text{Ar}^{+1}$  ions. In DC magnetron discharge, the major ion species were  $\text{Ar}^{+1}$  ions.

Thick Ta coatings, up 100  $\mu\text{m}$  thick, were successfully deposited on A723 steel substrates. The  $\alpha$ -phase Ta is preferred for high temperature wear and erosion applications. XRD showed Ta-2 and Ta-3 samples were bcc  $\alpha$ -Ta with Ta (110) texture, except Ta-1 has both  $\alpha$ - and  $\beta$ - Ta phases. Hardness values for Ta-2 and Ta-3 were  $\sim 8$ -9 GPa. For Ta-1, it was high at 12.9 GPa, due to the hard and brittle  $\beta$ -Ta component in the sample. In Figure 2, SEM topography and microstructure are shown for fractured surfaces of example Ta coatings on A723 steel: 55  $\mu\text{m}$  Ta deposited at -50 volt substrate bias (top); and 90  $\mu\text{m}$  Ta deposited at floating bias (bottom). Ta deposited at -50 volt substrate bias showed denser structure and finer grain size compared to Ta deposited at floating substrate bias. A layered structure was observed in the 55  $\mu\text{m}$  sample due to intentionally changing the pulsing characteristics during

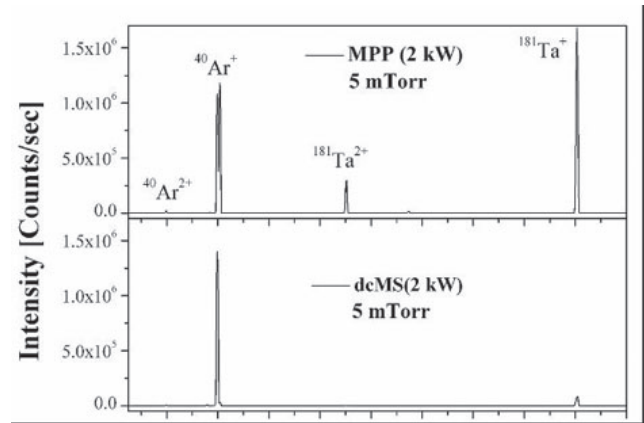
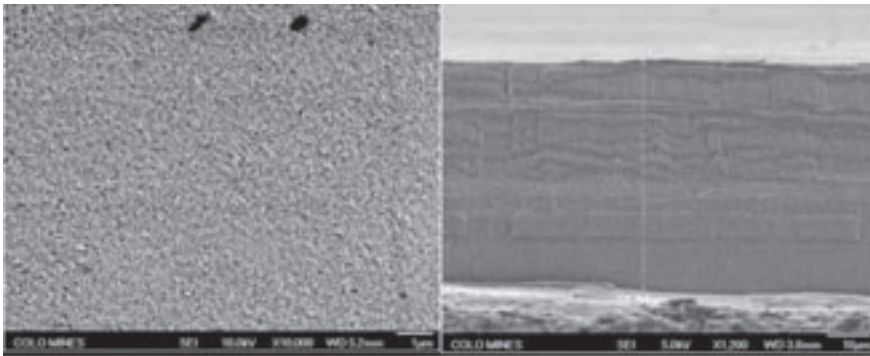
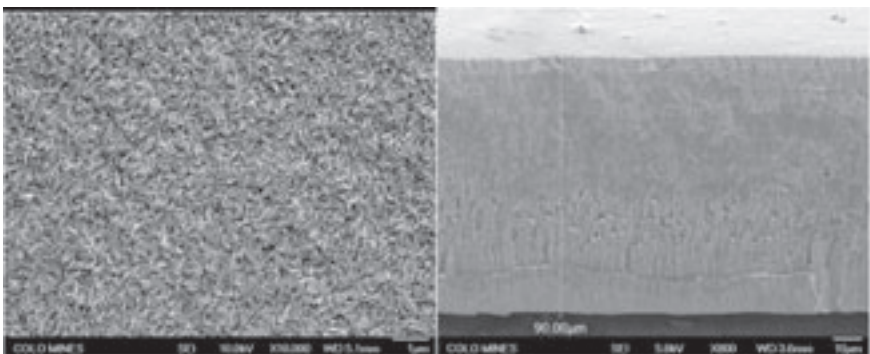


Figure 1: Mass-Ion distribution of plasma generated by a Zpulsor MPP powered magnetron at 5 mTorr argon, measured using an electrostatic quadrupole (EQP) mass spectrometer in a close field unbalanced magnetron system.

deposition. Residual stresses were evaluated using a TEC stress analyzer using Cr radiation reflecting from Ta (220) at  $\sim 107^\circ$  two-theta: High compressive residual stresses were detected: biased sample was  $-(2.8 \pm 0.4 \text{ GPa})$  or  $-(405 \pm 61 \text{ Ksi})$ ; floating sample was  $-(2.1 \pm 0.2 \text{ GPa})$  or  $-(307 \pm 25 \text{ Ksi})$ . Coating deposited at -50 volt bias had higher compressive residual stress compared to coating deposited at floating point bias, due to the higher energy ion bombardment. Errors in the residual stress measurement are from combined statistics error and the error of best fit using sin-square-psi technique.



a. SEM of 55  $\mu\text{m}$  MPP Ta deposited at -50 volt substrate bias.



b. SEM of 90  $\mu\text{m}$  MPP Ta deposited at floating substrate bias.

Figure 2: SEM topography and microstructure of fractured surface of Ta coatings deposited using MPP generated plasma: The biased sample showed denser structure with smaller grains compared to the coating deposited at floating substrate bias.



### Ta deposition in cylindrical geometry using DC and HIPIMS technology

In Table 2, Ta coatings were deposited on A723 steel samples in cylindrical geometry using DC unbiased, DC biased, HIPIMS unbiased, HIPIMS biased techniques. Ta coatings, 28-40  $\mu\text{m}$ , were deposited in 4 hrs at a deposition rate of  $\sim$ 8-10  $\mu\text{m/hr}$ . HIPIMS deposition rates were lower than DCMS. XRD showed that all samples were  $\alpha$ -Ta with Ta (110) texture, except Tacms3 consists of mixture of  $\alpha$ -Ta and  $\beta$ -Ta. Hardness measurements gave 5-8 GPa, except Tacms3, which was 11.6 GPa. It was harder due to higher energy bombardment using biased deposition and the presence of harder  $\beta$ -Ta in the coatings. Residual stress measured were in the range of  $-(1.52-1.79)\text{Mpa}$  or  $-(220-260)\text{Ksi}$  for the  $\sim$ 40 $\mu\text{m}$  coatings, slightly lower than stresses in the MPP deposited thicker coatings listed in Table 1.

In Figure 3, topography (top row at X250), microstructure (middle row at X10,000), topography (bottom row at X1,000) are compared for coatings deposited using DC and HIPIMS, unbiased and biased at -50 volt. DC deposited Ta showed larger grains and voids, either biased at -50 volt or unbiased; as HIPIMS deposited Ta showed more dense coatings with smaller grains. Biased HIPIMS deposition had smaller grains

compared to unbiased HIPIMS. However, the sample consisted of mixed phases of Ta, which could cause morphological variations. In Figure 4, a groove adhesion test (left) was performed, and no coating cracking or delamination was observed. In Figure 5, RC indentation test was performed (right). There were radial cracks in the HIPIMS depositions, but no cracks or failure was observed for areas under indentation.

### Ta deposition on interior surfaces of cylindrical structure

Thick Ta coatings up to 200  $\mu\text{m}$  have been successfully deposited directly on the interior surfaces of several 1 ft long cylinders of 120 mm diameter using biased DC and MPP technologies: Thick Ta coatings have been deposited at SWRI using biased DC cylindrical magnetron system and with MPP cylindrical magnetron at Benét. In Figure 5, nondestructive coating thickness mapping along cylinder axis are shown. Ignoring end effects at the cylinder ends, the dotted line represents a 106 $\mu\text{m}$  Ta-coated cylinder using MPP at zero substrate voltage. It had good thickness uniformity along the cylinder axis. The coating was  $\alpha$ -Ta with Ta (111) texture. In Figure 5, the solid lines represent a 130  $\mu\text{m}$  Ta-coated cylinder using biased DC. It showed good azimuthal thickness uniformity, but is thicker on one end compared to the other. Gas flow direction and plasma non-uniformity caused

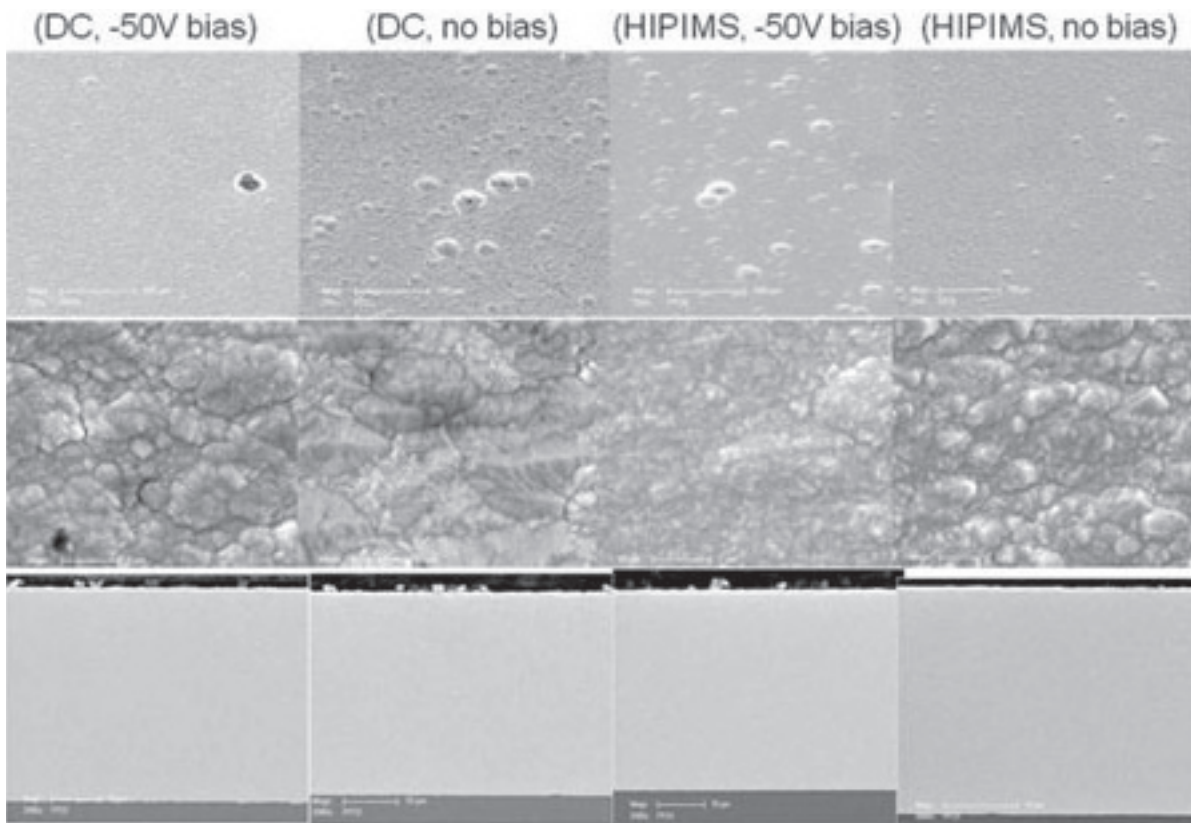


Figure 3: Ta depositions using cylindrical magnetron powered by: 1) DC with -50 volt bias, 2) DC no bias, 3) HIPIMS with -50 volt bias, 4) HIPIMS no bias: topography at 250x (top), topography at 10,000x (middle), microstructure at 1,000x (bottom).

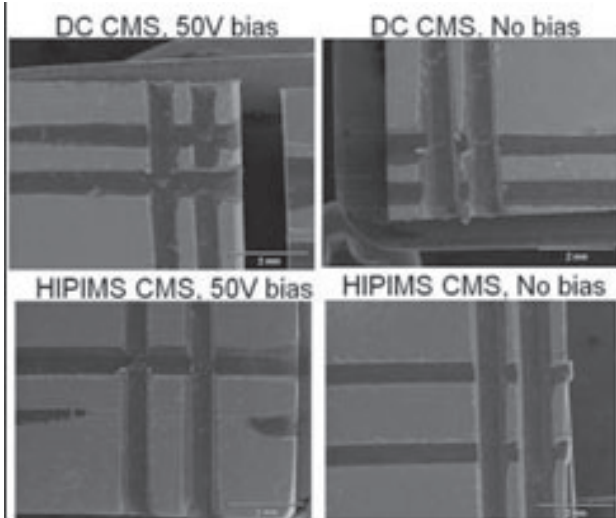


Figure 4: ASTM B571 groove adhesion test using a tungsten carbide tool (left) and RC Indentation test (right) of Ta deposited in cylindrical magnetron using DC and HIPIMS, unbiased and biased at -50 volt.

the thickness variation, which can be corrected by adjusting the magnet design or argon flow. The coating was  $\alpha$ -Ta with Ta (211) and Ta (111) texture. The cylinder deposited at -40 volt substrate bias using MPP was  $\beta$ -Ta, expected since MPP depositions resulted in a  $\beta$ - to  $\alpha$ - phase transition at -40 to -50 volt substrate bias voltage [21].

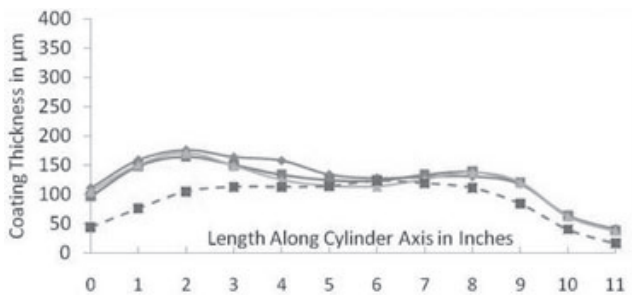
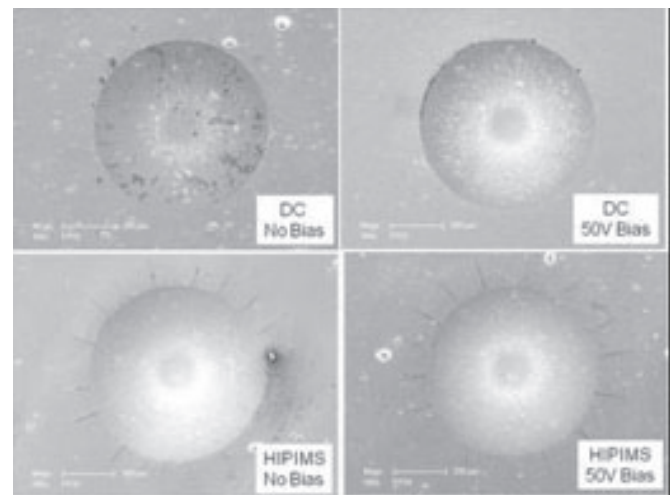


Figure 5: Nondestructive thickness mapping of Ta coated barrel sections along longitudinal axis: deposited using biased DC (solid lines at 3, 6, 9 o'clock); deposited using MPP (dotted line at 6 o'clock).

### Comparative Pulse laser heating test for MPP, PEMS, and electroplated HC Cr

Pulsed laser heating (PLH) test can access high temperature adhesion properties of coatings and materials [26]. PLH tests were performed for MPP and PEMS deposited Ta coatings in planar and cylindrical geometry. In Figure 6, PLH tests were performed using parameters: 2.5 msec, 1.0 J/mm<sup>2</sup> pulses, 20 cycles, to simulate the ~1460°C bore temperature. Ta samples deposited using plasma enhanced PEMS, MPP plasma in planar geometry, and MPP and biased DC in cylindrical geometry showed no cracking and no delamination, while extensive cracks were observed for HC Cr coatings, extending into the substrate to cause erosion and wear.



### CrN depositions in planar geometry using MPP technology

CrN forms in fcc phase CrN and hexagonal Cr<sub>2</sub>N phases depending on the N<sub>2</sub> percentage in the deposition system; Cr<sub>2</sub>N to CrN transition generally occurs at ~30-40% nitrogen-argon mix for DC and middle frequency pulsed DC magnetron sputtering [24]. In Table 3, CrN coatings with thicknesses in the range of 10- 55 µm were successfully deposited on 1020 steel using MPP technology. High deposition rates of 10 -15 µm per hour were obtained using a 3 kW average target power, a 50 cm substrate to target distance and an Ar/N<sub>2</sub> gas ratio of 1:1. Figure 7 shows the SEM cross section of the 12µm and 20 µm fractured surface. Dense coatings free of porosity and macro-particle incorporation were observed with good adhesion strength to the steel substrate.

To compare DCMS and MPP deposited coatings, 2.5 µm CrN coatings were deposited using DC and MPP at a -50 V DC substrate bias and an Ar/N<sub>2</sub> gas ratio of 1:1. In Figure 8, DCMS deposited CrN is shown on the left, MPP deposited CrN at -50 volt bias is shown on the right. XRD analysis showed that both coatings were the fcc CrN structure. It can be seen that the MPP CrN coating exhibits much denser structure and finer grain size than the DC CrN coating. This structural improvement of the MPP CrN coating as compared to the DC CrN coating is due to the enhanced ion bombardment from the highly ionized MPP plasma. The wear resistance of the CrN coatings deposited using DC and MPP techniques at different N<sub>2</sub> gas flow rate percentages is shown in Figure 9. The pin-on-disk wear tests were carried out by sliding against a 1 mm WC-Co ball at a 3N normal load and a 40 rpm rotation speed for 5000 cycles. In general, the MPP CrN coating showed lower coefficient of friction values than the DC CrN coating for a wide range of N<sub>2</sub> to Ar flow ratios, indicating their improved wear resistance due to the dense microstructure and smooth surface roughness using the MPP techniques.

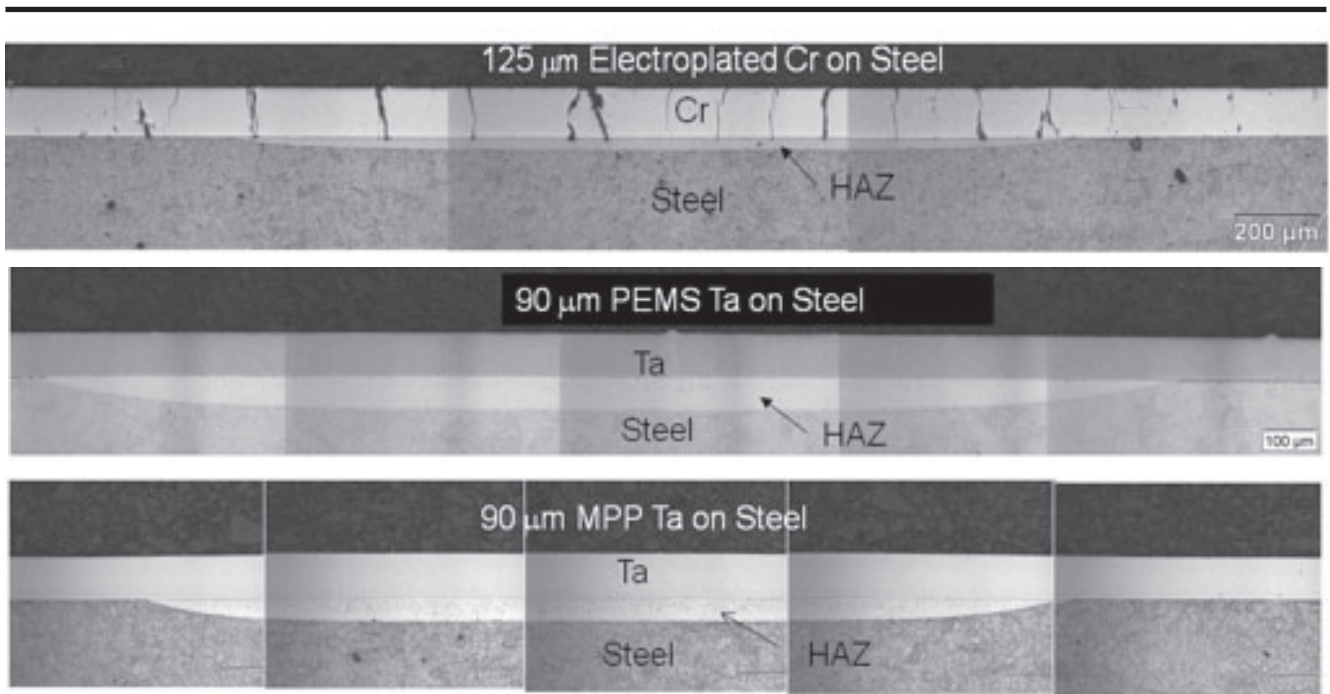


Figure 6: Comparative high temperature pulsed laser heating (PLH) at 1460°C; 1) Electroplated HC Cr on steel (row 1); 2) PEMS deposited Ta on steel (row 2); 3) MPP deposited Ta on steel (row 3). Heat affected zone (HAZ) in steel is due to tempered to untempered martensite conversion during the laser heating process.

Table 3: Planar magnetron chromium nitride deposition using MPP technology.

| Run   | Pa [kW] | Pp [kW] | Ia [A] | Ip [A] | Va [V] | Vp [V] | Pressure [mTorr] | Ar:N <sub>2</sub> [sccm] | Bias [V] | f [Hz] | Substrate distance [mm] | Time [hr] | Thick [μm] | phase |
|-------|---------|---------|--------|--------|--------|--------|------------------|--------------------------|----------|--------|-------------------------|-----------|------------|-------|
| CrN-1 | 3       | 95      | 83     | 190    | 463    | 575    | 5                | 25:25                    | -50      | 70     | 60                      | 1         | 12         | fcc   |
| CrN-2 | 3       | 95      | 83     | 190    | 463    | 575    | 5                | 25:25                    | -50      | 70     | 60                      | 2         | 20         | fcc   |
| CrN-3 | 3       | 95      | 83     | 190    | 463    | 575    | 5                | 25:25                    | -50      | 70     | 60                      | 4.5       | 50         | fcc   |

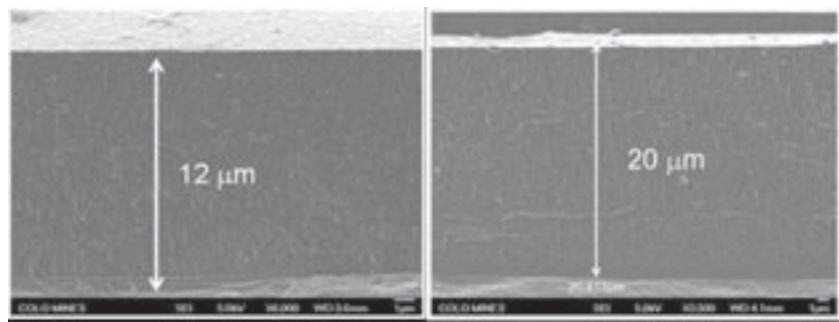


Figure: 7 SEM of microstructure of fractured surfaces of CrN coatings deposited using MPP generated plasma: 10 μm and 20 μm coatings showing dense adhesive coatings on steel.



## CONCLUSION

1. New technologies: High Power Impulse Magnetron (HIPIMS), Modulated Pulsed Power (MPP), and Plasma Enhanced Magnetron (PEMS) were tested to deposit improved coatings with dense micro-structures, smaller grains; improved topography and microstructure, less prone to crack formation compared to DC Magnetron (DCMS) and electroplated HC Cr coatings.

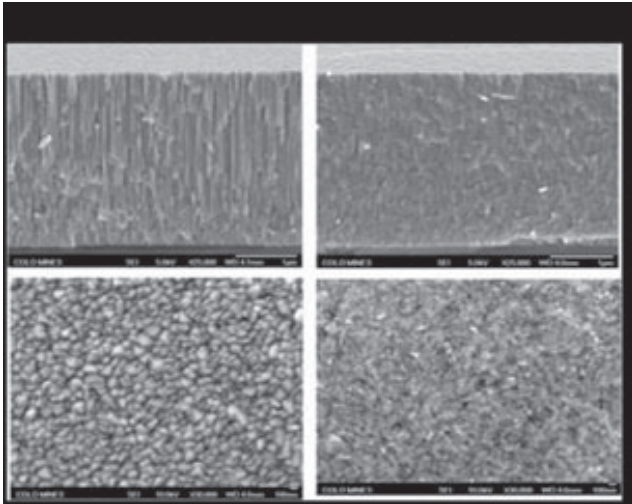


Figure 8: Comparison of DCMS-deposited CrN coatings (left) and MPP-deposited CrN coatings (right): coatings deposited at biased substrate are denser with smaller grains.

2. The bcc  $\alpha$ -Ta coatings, up to 200  $\mu\text{m}$ , were successfully deposited on A723 steel surfaces in planar and cylindrical geometries, and on the interior surfaces of 1 ft, 120 mm diameter cylinders using plasma generated by DCMS, PEMS, HIPIMS, and MPP processes. Groove tests, indentation tests, and high temperature pulse laser heating tests at 1450°C showed adhesive and crack-resistant coatings compared to electroplated HC Cr coatings.
3. The fcc CrN coatings, up to 55  $\mu\text{m}$  thick, were successfully deposited on steel in planar geometry using the MPP technology for wear-corrosion applications. The coatings exhibited dense microstructure, fine grain size, high hardness, and good adhesion and wear resistance properties. MPP deposited CrN showed better wear properties compared to DCMS deposited CrN coatings.
4. The new technologies have potential to deposit dense, adhesive, crack-resistant environmental friendly coatings, alternatives to chrome electroplating process.

## REFERENCES

1. V. Kouznetsov, K. Macák, J.M. Schneider, U. Helmersson, and I. Petrov, "A novel pulsed magnetron sputter technique utilizing very high target power densities," Surf. Coat. Technol., vol. 122, pp. 290-293, 1999.
2. A.P. Ehasarian, R. New, W.-D. Münz, L. Hultman, U. Helmersson, and V. Kouznetsov, "Influence of high power densities on the composition of pulsed magnetron plasmas," Vacuum, vol. 65, no. 2, pp. 147-154, 2002.

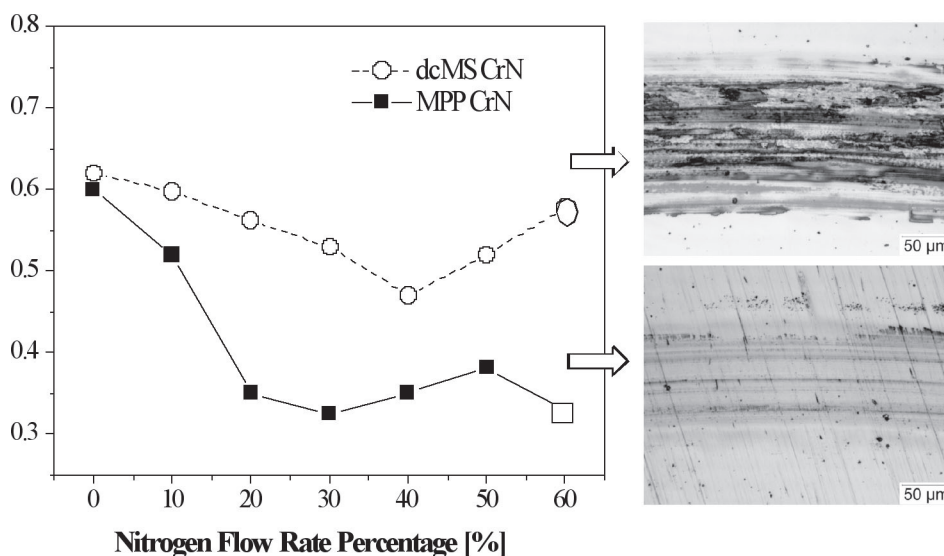


Figure 9: Comparison of coefficient of friction of CrN coatings deposited using DCMS and MPP technologies: MPP deposited coatings exhibited lower COF and better wear resistance compared to DC deposited CrN coatings.

3. U. Helmersson, M. Lattemann, J. Bohlmark, A. P. Ehiasarian, and J. T. Gudmundsson, "Ionized physical vapor deposition (IPVD): A review of technology and applications," *Thin Solid Films*, vol. 513, pp. 1-24, 2006.
4. Anders, J. Andersson and A. Ehiasarian, "High power impulse magnetron sputtering: Current-voltage-time characteristics indicate the onset of sustained self-sputtering," *J. Appl. Phys.*, vol. 102, p. 113303, 2007.
5. R. Chistyakov, B. Abraham, W. Sproul, J. Moore, J. Lin, "Modulated Pulse Power Technology and Deposition for Protective and Tribological Coatings," *50th Annual Technical Conference Proceedings of the Society of Vacuum Coaters*, p. 139, 2007.
6. R. Chistyakov, B. Abraham, W.D. Sproul, "Advances in High Power Pulsed Reactive Magnetron Sputtering," *49th Annual Technical Conference Proceedings of the Society of Vacuum Coaters*, p. 16, 2006.
7. J.N. Matossian, R. Wei, J. Vajo, G. Hunt, M. Gardos, G. Chambers, L. Soucy, D. Oliver, L. Jay, C. M. Taylor, G. Alderson, R. Komanduri and A. Perry, *Surf. Coat. Tech.*, Vol. 108-109, p. 496, 1998.
8. R. Wei, J.J. Vajo, J.N. Matossian, and M.N. Gardos, *Surf. Coat. Tech.*, Vol. 158-159, P. 465, 2002.
9. K. Truszkowska, M. Wotzak, F. Yee, G.N. Vigilante, and M. Cipollo, "Cylindrical Magnetron Sputter deposition of chromium coatings for erosion and wear resistant application," *47th Annual Technical Conference Proceedings of the Society of Vacuum Coaters*, p. 282, 2004.
10. J. Lin, J.J. Moore, W.D. Sproul, B. Mishra, and Z.L. Wu, "Modulated pulse power sputtered chromium coatings," *Thin Solid Films*, vol 518, p. 1566, 2009.
11. J. Alami, P. Eklund, J.M. Anderson, M. Lattemann, E. Wallin, J. Bohlmark, P. Persson, U. Helmersson, "Phase Tailing of Ta films by High Ionized Pulsed Magnetron Sputtering," *Thin Solid Films*, Vol. 515, 3434, 2007.
12. J. Alami, P.O. Persson, J.T. Gudmundsson, J. Bohlmark, U. Helmersson, "Ion-Assisted Physical Vapor Deposition for Enhanced Film Properties on Non-flat Surfaces," *J. Vac. Sci. Tech. A*, Vol. 23, No. 2, p. 278, 2005.
13. S. L. Lee, D. Windover, T. -M. Lu, M. Audino, "In situ phase evolution study in magnetron sputtered tantalum thin films," *Thin Solid Films* 420-421, p. 287, 2002.
14. L. Gladczuk, A. Patel, C. Singh Puar, M. Sosnowski, "Tantalum films for Protective Coatings of Steel," *Thin Solid Films*, 467, p. 150, 2004.
15. S. L. Lee, , M. Doxbeck, J. Mueller, M. Cipollo, P. Cote, "Texture, structure and phase transformation in sputter beta tantalum coating," *Surf Coat Tech*, Vol 177-178, p. 44, 2004.
16. Yee, M. Wotzak, M. Cipollo, and K. Truszkowska, "Cylindrical magnetron sputtering in a ferromagnetic cylinder," *47th Annual Technical Conference Proceedings of the Society of Vacuum Coaters*, p. 17, 2004.
17. C.P. Mulligan, S.B. Smith, G.N. Vigilante, "Characterization and comparison of magnetron sputtered and electroplated gun bore coatings," *J. of Pressure Vessel Tech.* 128, p. 240, 2006.
18. G.N. Vigilante and C.P. Mulligan, "Cylindrical Magnetron Sputtering (CMS) of coatings for wear life extension in large caliber cannons," *Materials and Manufacturing Processes* 21, p. 621, 2006.
19. S.L. Lee and R. Wei, "Effect of increased ion bombardment on magnetron sputtered refractory coatings," *50th Annual Technical Conference Proceedings of the Society of Vacuum Coaters*, p. 441, 2007.
20. S.L. Lee, R. Wei, E. Langa, M. Todaro, S. Smith, K. Coulter, "Plasma-enhanced sputtered Ta for barrel applications," *52nd Annual Technical Conference Proceedings of the Society of Vacuum Coaters*, p. 558, 2009.
21. S.L. Lee, M. Cipollo, F. Yee, R. Chistyakov, B. Abraham, "HIPIMS-MPP sputtered Ta films using I-PVD technology," *52nd Annual Technical Conference Proceedings of the Society of Vacuum Coaters*, p. 258, 2009.
22. T. Hurkmans, D.B. Lewis, H. Paritong, J.S. Brooks, W.D. Münz, "Influence of ion bombardment on structure and properties of UBM grown CrN coatings," *Surf. Coat. Tech.* 114, p. 52, 1999.
23. A.P. Ehiasariana, P. Eh. Hovsepiana, L. Hultmanb, U. Helmersson, "Comparison of microstructure and mechanical properties of chromium nitride-based coatings deposited by high power impulse magnetron sputtering and by the combined steered cathodic arc/unbalanced magnetron technique," *Thin Solid Films* 457, p. 270-277, 2004.
24. J. Lin, Z.L. Wu, X.H. Zhang, B. Mishra, J.J. Moore, W.D. Sproul, "A comparative study of CrN coatings synthesized by DC and pulsed DC magnetron," *Thin Solid Films* 517, p. 1887, 2009.



- 
25. J. Lin, J.J. Moore, W.D. Sproul, B. Mishra, Z. Wu, J. Wang, "The structure and properties of chromium nitride coatings deposited using dc, pulsed dc and modulated pulse power magnetron," *Surf. Coat. Tech.* 204, p. 2230, 2010.
26. P.J. Cote, M. Todaro, G. Kendall, "Laser Pulse Heating of Gun Bore Coatings," *Surf. Coat. Tech.* 146-147, p. 65, 2001.